

Reactive Power Flow Optimization in the presence of Secondary Voltage Control

Valentin Ilea, Cristian Bovo, *Member, IEEE*, Marco Merlo, Alberto Berizzi, *Member, IEEE*, Mircea Eremia, *Senior Member, IEEE*

Abstract-- The Hierarchical Voltage Control has recently become an important alternative to the traditional voltage control solutions. This paper deals with the computation of an optimal profile for the pilot bus voltages using different optimization strategies. For this purpose, the mathematical model of the optimization problem was studied considering two issues: *i)* defining the constraints of the optimization problem in order to fulfill the actual operating condition of the Secondary Voltage Control system and *ii)* finding the proper objective function (OF). For validation, tests were made on the Italian Power grid by using the high level modeling system GAMS.

Index Terms-- complementary constraints, hierarchical voltage control, optimal reactive power flow, security.

I. INTRODUCTION

THE control of voltages and reactive power has become more and more critical in the power system operation, in recent years, due to the presence of the electricity market that pushes system operators and electrical utilities to operate the transmission networks as close as possible to their maximum capacity [1]. To improve voltage control in transmission grids, many projects have been developed around the world. The Hierarchical Voltage Control System (HVCS), which is based on network area and resources subdivision, although developed by vertically integrated utilities in the past, is widely recognized as a viable solution and was adopted in several countries around the world [2].

Generally HVCS is made by a primary level (primary voltage control – PVC) given by the generators AVRs (Automatic Voltage Regulator), a secondary voltage control level (SVC) and a tertiary voltage control level (TVC) [2] (Fig. 1).

The Secondary Voltage Control (SVC) exploits a network subdivision into electric areas around the so-called pilot buses, representative for the voltage profile of the area load buses.

Each pilot bus is regulated by the most effective area generators – the control generators – by changing their reactive output according to the area reactive level q (the ratio between the supplied reactive power and the maximum value of the reactive power that the control generators can supply in each area). Thus, an equal reactive loading of all the control generators in each area is achieved. The adjustment of each generator is locally accomplished by acting on the set-points of the AVRs; this is performed, for each control area, by a secondary voltage regulator (SVR).

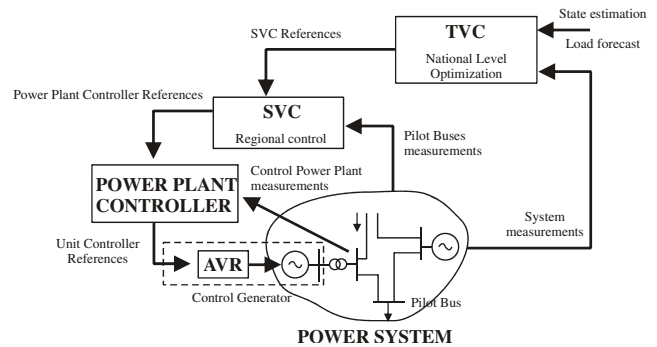


Fig. 1. Structure of the hierarchical voltage – reactive power control system

The TVC provides a further closed control loop and coordinates the actions of the SVRs by computing the values of the set-points of the pilot bus voltages on the basis of the optimization carried out on the load forecast and on the output of the state estimator.

The purpose of this paper is to adapt the Optimal Reactive Power Flow (ORPF) problem to power systems with SVC in order to improve the operation and security [3] of such networks. The main goal is to compute an optimal voltage profile for the pilot buses using different optimization strategies and to select the most suitable one.

II. MATHEMATICAL MODEL OF THE ORPF

Generally, the mathematical model of an optimization problem is given by an objective function (OF) to be minimized (or maximized) together with the constraints to which it is subjected:

$$\begin{aligned} \min f(x) \\ \text{subject to } a \leq g(x) \leq b \\ l \leq x \leq u \end{aligned} \quad (1)$$

where $f(x)$ is the objective function, x is the vector of variables and the constraints of the problem are specified.

V. Ilea is with the Energy Department, “Politecnico di Milano”, Via La Masa, MI 20156, Italy and with Power System Department, University “Politehnica” of Bucharest, Spl. Independentei, No. 313, Bucuresti, Romania (e-mail: ileav2003@yahoo.com).

C. Bovo is with the Energy Department, “Politecnico di Milano”, Via La Masa, MI 20156, Italy (e-mail: cristian.bovo@polimi.it).

M. Merlo is with the Energy Department, “Politecnico di Milano”, Via La Masa, MI 20156, Italy (e-mail: marco.merlo@polimi.it).

A. Berizzi is with the Energy Department, “Politecnico di Milano”, Via La Masa, MI 20156, Italy (e-mail: alberto.berizzi@polimi.it).

M. Eremia is with Power System Department, University “Politehnica” of Bucharest, Spl. Independentei, No. 313, Bucuresti, Romania (e-mail: eremia1@yahoo.com).

Thus, we have direct constraints on variables and constrained functions $g(x)$ which contain the variables of the problem.

A. Objective functions

Depending on the optimization strategy chosen, different objective functions were implemented [3] – [5]:

a) *Minimizing real power losses* (min los): this optimization problem consists in minimizing the sum of the real power losses in the branches of the network. In a liberalized market environment, the real power generation is contracted and hence, from our point of view, it is fixed. With this assumption, minimizing the real losses is equivalent to minimization of the real power produced by the slack generator:

$$\min P_{SL} \quad (2)$$

where P_{SL} is the real power at the slack bus.

This methodology is currently used by system operators worldwide and its goal is to reduce the operating costs associated with the power losses. The security is implicitly guaranteed by the respect of the operational limits [3].

b) *Minimizing the reactive power produced/absorbed by the generators* (min Qg^2): the objective is to determine an optimal point in which the generators have a wide regulation margin, granting the power system a significant reserve of reactive resources against possible perturbations:

$$\min \sum_i Q_{g,i}^2 \quad (3)$$

where i refers to all generators.

This function is suitable to fulfill the liberalized energy markets requirement to give attention to costs related to the optimal dispatch of reactive power resources. With this strategy, the goal is to obtain a better distribution of the reactive power margins over the system [3], and concerning security, we have an indirect control: in case of contingency the generators will have greater regulation margins to restore a secure operating condition.

c) *Maximizing the loadability* (max L): it consists in maximizing the loadability factor λ seen as the distance of the current operating point from the point of collapse of the network (e.g., the critical point of the PV curves) [4] – [7]:

$$\max \lambda \quad (4)$$

The implementation of this function assumes a load increase in every PQ bus j described by:

$$P_{Dj,\lambda} = P_{Dj,0} + \lambda P_{Dj,0} \quad (5)$$

where;

$P_{Dj,0}$ is the initial load;

$P_{Dj,\lambda}$ is the load value for a given λ .

In the proposed model, to stress in a realistic way the

system, also an increase in the reactive power of the load has been introduced:

$$Q_{Dj,\lambda} = Q_{Dj,0} + \lambda P_{Dj,0} a \quad (6)$$

where a is a constant parameter derived from the imposed power factor. In the cases presented in the paper, we chose a constant power factor 0.9 in every bus, and thus:

$$a = \tan(\arccos(0.9)) \quad (7)$$

Since we are increasing the load, it is also necessary to consider a corresponding increase in the real power generation:

$$P_{Gi,\lambda} = P_{Gi,0} + \lambda \Delta P_{Gi} \quad (8)$$

where ΔP_{Gi} represents the increase of power generation at each generator except the slack generator, since it must compensate the changes of the system losses. Therefore:

$$\Delta P_{Gi} = b \beta_i \lambda \sum_j P_{Dj,0} \quad (10)$$

where b is necessary to approximately compensate the increase in the real power losses due to load increase and β_i defines the participation of generator i to the total generation change. Typically, b assumes values between 1.01 ÷ 1.05 while β_i is computed as:

$$\beta_i = \frac{P_{Gi,\max} - P_{Gi}}{\sum_i (P_{Gi,\max} - P_{Gi})} \quad (11)$$

Moreover, thanks to of the definition of β_i , each generator is loaded according to its margin.

As for the generated reactive power, it is not necessary to define a pattern for its increase, since its value is an output of the power flow equation solution.

This OF is specially designed to optimize the security of the network as it allows us to maximize the “distance” between the actual operating point and the collapse one.

B. ORPF constraints

All the above functions a), b) and c) are subject to equality constraints given by the power flow equations:

$$P_k - \sum_{m=1}^N V_k V_m Y_{km} \cos(\theta_k - \theta_m - \phi_{km}) = 0, k=1\dots N \quad (12,a)$$

$$Q_k - \sum_{m=1}^N V_k V_m Y_{km} \sin(\theta_k - \theta_m - \phi_{km}) = 0, k=1\dots N \quad (12,b)$$

to which we add the SVC conditions [1], [8]:

$$\begin{aligned} \frac{Q_1^r}{Q_{1,\max}^r} &= \dots = \frac{Q_k^r}{Q_{k,\max}^r} = \dots \\ &= \frac{Q_{n_c^r}^r}{Q_{n_c^r,\max}^r} = q_r, i=1\dots n_c^r \quad r=1\dots n_a \end{aligned} \quad (13)$$

where:

P_k is the active nodal power at bus i ;

Q_k is the reactive nodal power at bus i ;
 N is the number of buses in the system;
 n_a is the number of control areas;
 j is the index of the control generators in area r ;
 n_c^r is the number of control generators in area r ;
 q_r is the reactive level of area r ;
 and the subscript *max* denotes the upper capability limit.

The OFs are also subject to inequality constraints given by the bus voltage magnitudes limits and the capability limits of the generators:

$$V_{k,\min} \leq V_k \leq V_{k,\max}, k \in \mathbf{VC} \quad (14,a)$$

$$Q_{Gi,\min} \leq Q_{Gi} \leq Q_{Gi,\max} \quad (14,b)$$

where:

\mathbf{VC} is the set of voltage constrained buses and holds all the load and the SVC control generator nodes;

$V_{k,\min/\max}$ are the lower/upper bounds of the bus voltage magnitudes, V_k ;

$Q_{Gi,\min/\max}$ are the lower/upper bounds of the supplied reactive power, Q_{Gi} .

Concerning the treatment of generators, for the ones not participating to SVC we chose to maintain the control on the voltages, while for the SVC control generators the attention is focused on the reactive power production needed to control the pilot node voltage, which is the main goal of the control scheme. Thus, the first set of generators is modeled as PV bus type while the generators in the second set are modeled as P-bus type. The P-bus type is a special bus type defined to solve the power flow (PF) problem in the presence of SVC [9]. In a PF, for the P – type, two equations are written: the first regards the real power (12, *a*), while the second one represents the alignment condition that characterizes the SVC (13). Moreover, the pilot bus is modeled as a PVQ type and it is seen as a PQ bus with the voltage magnitude fixed. For our optimization problem, the voltage of the pilot bus is an independent variable.

A typical problem of modeling PV buses is the sudden change to PQ when the generators hit their capability limits; in our approach, this switch is modeled with the help of complementarity constraints [10], which have a disjunctive character allowing thus the system to behave according to different rules under different circumstances without using different models:

$$\begin{aligned}
 (Q_{Gi} - Q_{Gi,\min}) \Delta V_i &\leq 0 \\
 (Q_{Gi} - Q_{Gi,\max}) \Delta V_i &\leq 0 \quad i \in \mathbf{PV} \\
 V_i &= V_{i,0} + \Delta V_i
 \end{aligned} \quad (15)$$

where ΔV_i is the change in voltage of the i th PV bus when one of the reactive limits is reached.

Therefore, depending on the operating mode of the

generator, the following situations can occur:

a) **NON-LIMITED MODE:** $Q_{Gi} - Q_{Gi,\min} > 0$ and $Q_{Gi} - Q_{Gi,\max} < 0$, thus $\Delta V_i \leq 0$ and, at the same time, $\Delta V_i \geq 0$ forcing ΔV_i to be zero. Thus, by the last equation of (15), the voltage of the generator is fixed to its set value;

b) **UNDER-EXCITED LIMITED:** $Q_{Gi} = Q_{Gi,\min}$ and thus the second equation of (15) forces $\Delta V_i \geq 0$. As consequence, $V_i \geq V_{i,0}$;

c) **OVER-EXCITED LIMITED:** $Q_{Gi} = Q_{Gi,\max}$ and thus the first equation of (15) forces $\Delta V_i \leq 0$. As consequence, $V_i \leq V_{i,0}$.

In this way, the actual behavior of the generator is achieved in a simple manner, using a single model for all situations.

While the above constraints apply to all three OFs, further constraints are necessary for the solution of the problem c), i.e. $\max \lambda$. In particular, we must define two sets of PF equations instead of one. The first set, which is given by equations (12), holds for the initial equilibrium point of the system, where $\lambda = 0$. The second set of equations is necessary to define the equilibrium point at $\lambda > 0$. This time, the nodal real and reactive powers are no longer constant but they are function of λ , according to equations (5), (6) and (10). Therefore, the following equality constraints must be fulfilled; this results in a doubling of the set of variables:

$$P_{cr,k} - \sum_{m=1}^N V_{cr,k} V_{cr,m} Y_{km} \cos(\theta_{cr,k} - \theta_{cr,m} - \phi_{km}) = 0 \quad (16,a)$$

$$Q_{cr,k} - \sum_{m=1}^N V_{cr,k} V_{cr,m} Y_{km} \sin(\theta_{cr,k} - \theta_{cr,m} - \phi_{km}) = 0 \quad (16,b)$$

where subscript *cr* represents the “doubled” set of variables.

In the same manner, equations (13) – (15) will be defined also for the critical variables.

When maximizing λ , we initially made the assumption that the security must be correlated with the controllability of the network. In this regard, the equality between the magnitudes of the pilot bus voltages in the initial and critical equilibrium points should be introduced as a supplementary constraint. But, in this way, when a secondary control area reaches saturation, i.e. the control is lost ($q_{crj} = 1$), the optimization process stops and λ can not be further increased.

Another possible choice is to allow the j -th pilot bus voltage to decrease when $q_{crj} = 1$; this can be done through additional complementarity constraints:

$$\begin{aligned}
 (1 - q_{cr,r}) \Delta V_{cr,r} &\leq 0 \\
 V_{cr,r} &= V_r - \Delta V_{cr,r} \quad r \in \mathbf{PVQ} \\
 \Delta V_{cr,r} &\geq 0
 \end{aligned} \quad (17)$$

where:

\mathbf{PVQ} is the set of pilot buses;

$\Delta V_{cr,r}$ is the change in voltage of the j -th pilot bus, when in the critical operating condition, its area reaches saturation.

It should be noted that by maximizing λ we do not obtain the mathematical critical point MCP (the nose of the PV curve) but a practical critical point, corresponding to the minimum limits imposed to the voltage profile (Fig. 2). This approach is reasonable since the operation of the system below the voltage limits is not a technically viable solution.

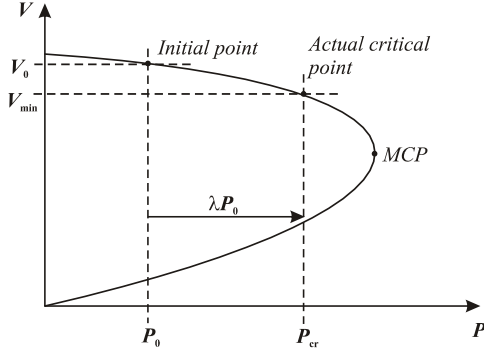


Fig. 2. Representation of the computed critical point.

Finally, we studied the relations and interactions between the proposed OFs by constructing multi-objective functions [11] (MOF) as linear combinations of single OFs. Such a MOF can be generally defined by:

$$\min \sum_i \alpha_i f_i \quad (18)$$

where:

f_i is the i th OF included in the MOF;

α_i is the weight of f_i in the MOF with $0 \leq \alpha_i \leq 1$ and

$$\sum_i \alpha_i = 1.$$

For the particular case of two OF equation (18), can be written as:

$$\min \alpha f_1 + (1-\alpha) f_2 \quad (19)$$

III. TESTS AND RESULTS

The above mathematical model was implemented in GAMS [12], a powerful tool for solving optimisation problems. To solve the problem, GAMS calls the internal solver COINOPT that uses a *primal-dual infeasible interior point method*. This, in his turn, uses PARDISO [13], [14] for the linearized part of the problem.

Two configurations of the Italian transmission system were used for testing: “Case A” and “Case B”. The two networks are identically divided into 13 control areas (see Fig. 3), but their loading is different: the first one is characterized by a medium load of around 30100 MW (“Case A”) while the other is operating under more stressed conditions with a load level of about 34400 MW (“Case B”); this is the equivalent load as seen by the EHV grid.

The Italian grid is characterized by a highly meshed network and high generation capability but also by a high load

in the north and north-center parts. The center part of the system is characterized by high loads around the big cities and by a couple of HV transmission lines connecting the power plants in the south to the high load areas. The center and south region are less loaded and meshed than the north. The system consists of around 1000 buses, 1100 branches and 180 generators of which almost half are control generators, so the model is complex and “realistic”, useful to describe the response of the Italian transmission network.

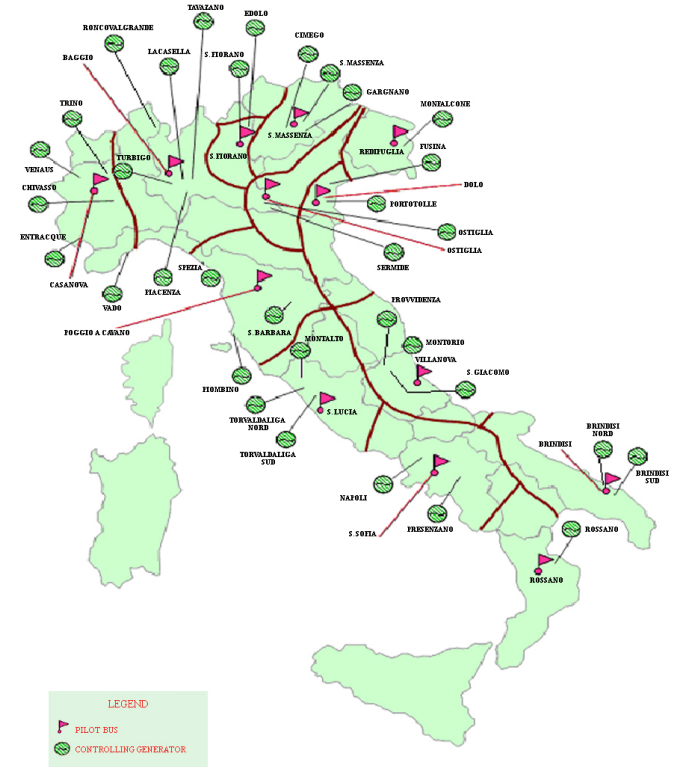


Fig. 3. Italian transmission system control areas.

A. “Case A”

Fig. 4 shows the voltage profiles for the pilot buses obtained for “Case A” for all the three proposed strategies. Table I gives the values of the OF and the total reactive power produced by the control generators in all situations, while in Fig. 5 the area reactive levels are depicted.

Initially, we will focus on the first two strategies since both are not directly connected with network security.

We notice that minimizing the power losses produces higher voltages and reactive effort than minimizing reactive generation. This is because the losses are directly dependent on the voltage level of the system and minimizing them requires a high voltage profile, and thus a high reactive effort from the generators. However we still have a large regulation margin available in the most important areas of the network for ‘min los’ (Fig. 5): Casanova and Baggio in the north with 2800 MVAR, Poggio and S. Lucia in the center with 3600 MVAR and Rossano and Brindisi in the south with 1600 MVAR. Moreover, Baggio has the highest reactive level of $q \approx 54\%$ which is quite comfortable.

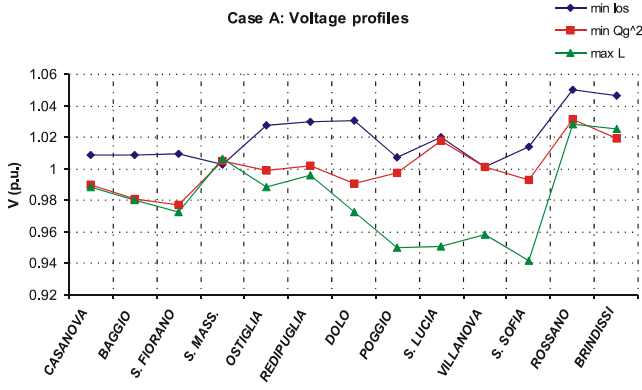


Fig. 4. Pilot bus voltage profiles for “Case A”

TABLE I
GLOBAL PARAMETERS FOR “CASE A”

	ΔP [MW]	$\Sigma Q_g P$ [MVar]	λ [-]	ΣQ_g^2 [p.u.]
min los	326	4712	-	0.411
min Q_g^2	337	3515	-	0.209
max L	357	4370	0.276	0.431

We also notice, in the north part of the system, regions where the voltage profile is flat for minimum losses. This is because, as mentioned earlier, the north region is highly meshed and thus there is a reactive coupling among areas. The south part of the system has the highest voltage level since it is mainly a generation region.

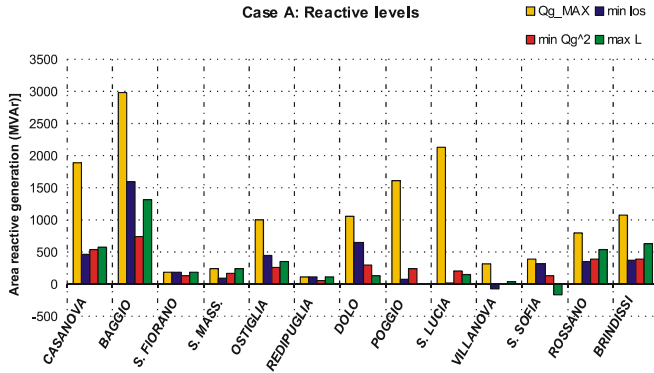


Fig. 5. Area reactive levels for “Case A” in the optimized operating points

Minimizing the total reactive power does not produce, in respect to ‘min los’, a high increase in the real power losses (≈ 12 MW or 3.6 % – see Table I). At the same time, the total reactive generation, represented in Table I by the value of the OF ‘ Q_g^2 ’, is almost reduced to half: 0.209 p.u. compared to of 0.411 p.u. Finally, from Fig. 5 we see that the major reduction in the reactive production of the control generators is due to the Baggio area, where we have a difference of 865 MVar compared to the difference of 1200 MVar that characterizes the whole Italian system. We can anticipate a conclusion by saying that, from the point of view of the

control generators production, the effect of minimizing reactive power in respect to losses minimization is mainly observed in the area with the most reactive power capability in the north (Baggio): actually, the losses minimization is performed by the exploitation of the whole reactive capability of the area. In the areas in the center, the differences are smaller and this results in a very high regulation margin.

Concerning the third optimization strategy, we obtained $\lambda \approx 0.276$ (see Table I) which is approximately 8500 MW of load margin to the critical point. The value is quite high, but it is reasonable since the system is not operating under stressed conditions. If we look at the voltage profile in Fig. 4 we notice a voltage profile lower than the other OFs, especially for the central part of the system. This is because the optimization is made under the assumption of equality between the pilot bus voltages in the initial point and in the critical point as long as some regulation margins are available. Thus, from Fig. 6 we see that in the respective areas we still have control over area reactive resources and hence, under high load margin conditions, the voltages are very low.

Finally, the low voltage profile determined high reactive losses in the branches of the grid resulting in higher real power losses (357 MW) and high reactive generation comparable to minimum losses case (see Table I). Nevertheless we have, like in the previous cases, a high regulation margin in the areas with the largest reactive capability (Fig. 5).

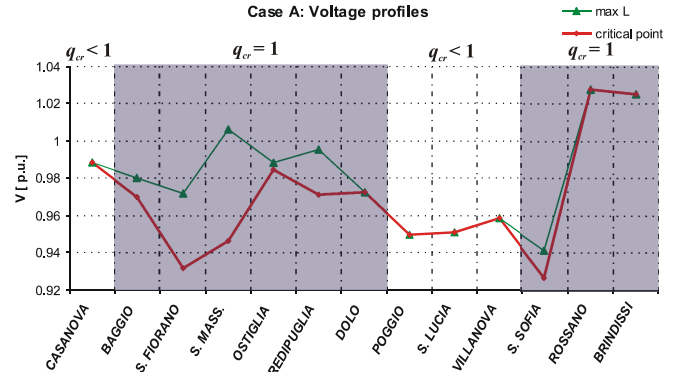


Fig. 6. Saturated areas and voltage profiles in the critical point for “Case A”.

B. “Case B”

Fig. 7 shows the voltage profiles for the pilot buses obtained for “Case B” for all the three proposed strategies. Table II gives the values of the OF and the total reactive power produced by the control generators in all tests, while in Fig. 8 the area reactive levels are depicted.

We observe in Fig. 7 that the profiles obtained in “Case B” are closer to each other than for “Case A”. We notice almost identical voltage levels in the center and south regions, while differences appear in the north region of the system. This is explained by the increased level of stress (≈ 4000 MW difference of load) in the network that results in reduced reactive resources available for the optimization: the lower

degrees of freedom are the cause of the similarity of the voltage profiles obtained with different optimization procedures. This also causes the similar values of losses computed for the different strategies; in any case, the losses are higher than in “Case A” because of the higher load of the system

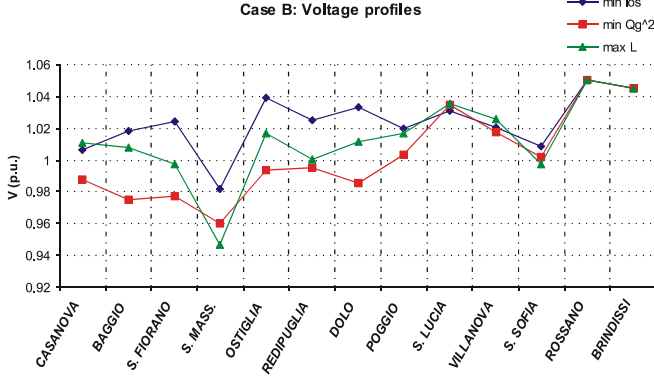


Fig. 7. Pilot bus voltage profiles for “Case B”

TABLE II
GLOBAL PARAMETERS FOR “CASE B”

	ΔP [MW]	$\Sigma Q_{g,p}$ [MVar]	λ [-]	ΣQ_g^2 [p.u.]
min los	423	5941	–	0.589
min Q_g^2	440	4864	–	0.325
max L	431	5826	0.127	0.550

As in the previous case, we again notice that the effect of minimizing reactive power in respect to losses is mainly observed in the Baggio area (≈ 1000 MVar with respect to the difference in the whole system of ≈ 1100 MVar) while in the center area the reactive level is very low and not much different ($q \approx 15\%$ for S. Lucia and $q \approx 30\%$ for Poggio). Nevertheless, even if the network is under high stress, we still have wide regulation margins no matter the optimization strategy applied (minimum losses or reactive generation).

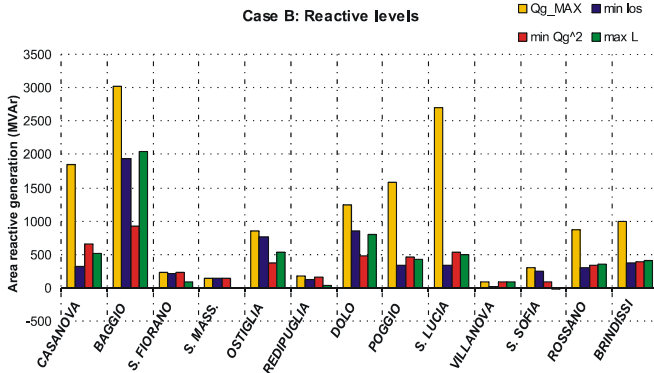


Fig. 8. Area reactive levels for “Case B” in the optimized operating points

Concerning the third OF, we obtain a lower loadability of $\lambda \approx 0.127$ (see Table II) which is related to the higher initial load level of the network and to the decreased control capability. Indeed, this is equivalent to an effective load margin of ≈ 4400 MW which is nearly half of the previous

case and more or less equal to the load level difference between the two systems (4300 MW). The reduced loadability also explains why the voltage level obtained with this strategy is not the lowest one.

Fig. 9 depicts a comparison between the optimal voltage profile ($\lambda=0$) and the critical voltage profile ($\lambda=0.127$) for “Case B”, together with the indication of the saturated control areas. This time, the difference between the optimal and the critical profiles is tight, reasonable for such a stressed network.

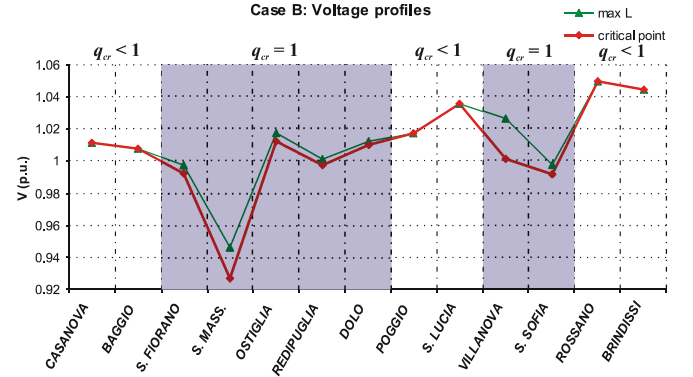


Fig. 9. Saturated areas and voltage profiles in the critical point for “Case B”.

As a general conclusion of the comparison of both cases, we can say that, from the point of view of SVC reactive resources, the OFs action is most noted in the Baggio area. Moreover, no matter the adopted strategy, the reactive level in Casanova area in north and in Poggio and S. Lucia areas in the center tends to be low so there will always be a high reactive reserve available. In the south (Rossano and Brindisi areas) the reactive production always maintains high the voltage levels permitting high power transits towards the rest of the system.

C. Multi-objective functions

Fig. 10 shows the curves for minimum losses – minimum reactive generation combination for both test systems. The simulations were made for the entire range of α with a step of 0.05. The curves show that the two strategies are in conflict. On one hand, for high weights on minimum losses (0.8 – 1) minimum reactive generation acts without a significant change in the value of losses. Then, on the other hand, for weights from 1 to 0.2 on reactive production OF, we notice the action of losses minimization proportional to its weight while the reactive generation OF is close to its optimal value.

Fig. 11 illustrates the curves for minimum losses – minimum λ combination for both test systems. This time, the simulations were performed for $\alpha=0.1 - 0.9$ with a step of 0.1.

As in the previous case, we notice again that the two strategies are in conflict. This time, in “Case A”, for $\alpha \geq 0.7$ the values of the OFs increase significantly and the losses distance themselves from the optimal value, while with the further decrease of α , λ stays near its optimal value and losses take control.

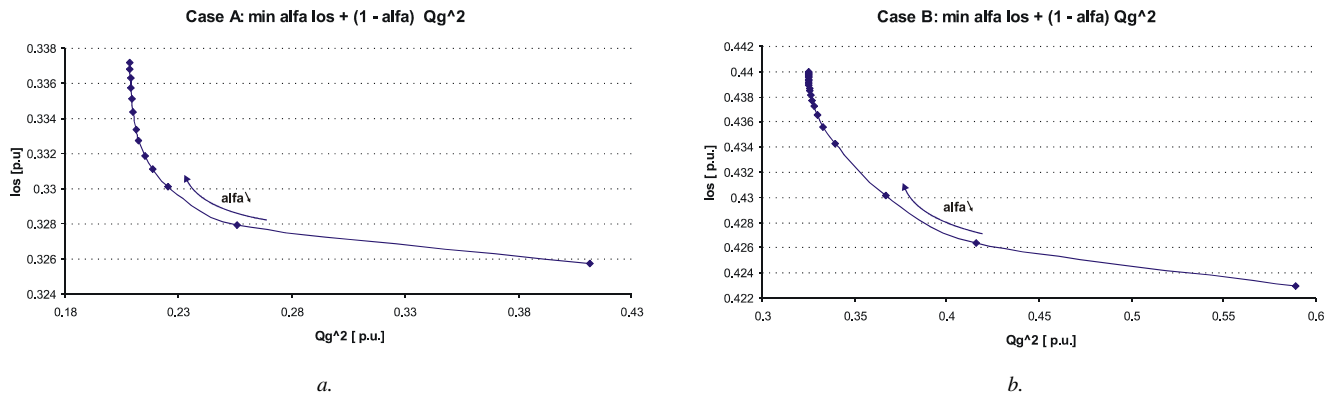


Fig. 10. min losses – min reactive generation: *a.* “Case A”; *b.* “Case B”.

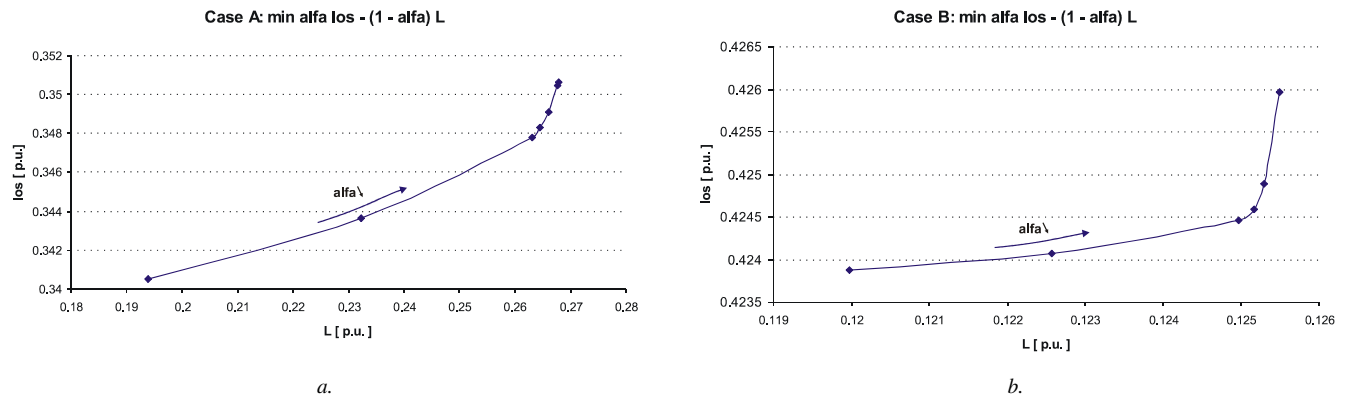


Fig. 11. min losses – max loadability: *a.* “Case A”; *b.* “Case B”.

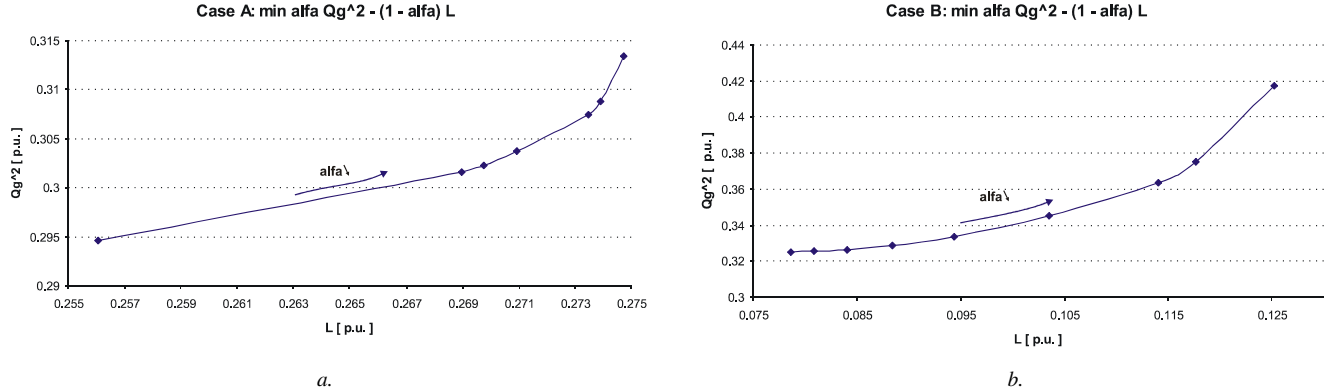


Fig. 12. min reactive generation – max loadability: *a.* “Case A”; *b.* “Case B”.

In “Case B” the situation is different: the losses are maintained near the optimum $\alpha \geq 0.7$ while λ augments until gets in the proximity of its optimum (for $\alpha \approx 0.7$), point from where the losses increase according with the diminish of their weight.

Fig. 12 illustrates the curves for the last possible combination: minimum reactive generation – minimum λ combination with $\alpha = 0.3 - 0.9$ with a step of 0.1. In “Case A” λ is in the proximity of the optimum for $\alpha \leq 0.8$ allowing the reactive generation to take control, while in “Case B” for $\alpha \geq 0.4$ the reactive production stays near its optimum. The MOF behavior is more unpredictable than in the previous cases.

Analyzing these situations, we may add that an optimal compromise between the two strategies, i.e. the proper MOF

combination and weights, not only depends on system characteristics (the form of the curves) but is also a decision of the Transmission System Operator (TSO). This chose the proper weights in accordance to its own requirements and to the energy market characteristics. For this, the TSO should define a set of practical rules that fulfill the above requirements and make them public.

IV. CONCLUSIONS

With this paper we have tested different ORPF strategies under the presence of SVC: the traditional active losses minimization currently used by the majority of TSOs worldwide and two other proposals, i.e. minimization of the generated reactive power and the loadability maximization.

Comparative tests were made on a “realistic” network model representing the Italian transmission system and the main characteristics of these strategies were emphasized for this particular grid.

Moreover, we have emphasized the conflictual relations between these OFs through MOF simulations. With this analysis, the TSO can make a compromise between different optimization strategies taking into account the actual market conditions. In other words, the TSO can choose the proper OFs to be mixed in the MOF and the optimal weights.

As future development one should focus the attention on verifying the security level offered by the proposed OFs. However, past studies showed that minimizing losses offers a better profile than minimizing reactive generation from the security point of view.

V. REFERENCES

- [1] A. Berizzi, C. Bovo, M. Delfanti, M. Merlo, G. Dell’Olio, M. Pozzi, *Coordination of the Hierarchical Voltage Control with the Reactive Power Economic Compensation*, IEEE PowerTech Conference, St. Petersburg, Russia. 27-30 June 2005.
- [2] S. Corsi, M. Pozzi, C. Sabelli, A. Serrani, *The coordinated automatic voltage control of the Italian transmission grid*, IEEE Transactions on power systems, vol. 19, no. 4, November 2004.
- [3] A. Berizzi, C. Bovo, M. Delfanti, M. Merlo, C. Bruno, M. Pozzi, *ORPF Procedures for Voltage Security in a Market framework*, IEEE Power Tech 2005, St. Petersburg, Russia. 27-30 June 2005.
- [4] A. Berizzi, C. Bovo, M. Delfanti, M. Merlo, D. Cirio, M. Pozzi, *Online fuzzy voltage collapse risk quantification*, Electric power system research, ISBN: 978-1-60692-613-0, 2008.
- [5] V. Ilea, A. Berizzi, M. Merlo, C. Bovo, M. Eremia, *Implementation of various objective functions for reactive optimal power flow in the presence of the hierarchical voltage control system*, 1st International Conference on Modern Power System, Cluj, Romania, November, 2006.
- [6] W. Rosehart, C. Canizares, V. Quintana, *Costs of voltage security in electricity markets*, IEEE PES Summer Meeting, Vol. 1, Seattle, July 2000.
- [7] A. Berizzi, C. Bovo, C. Canizares, W. Rosehart, *Comparison of voltage security constrained optimal power flow techniques*, IEEE PES Summer Meeting, Vancouver (BC), Canada, 15-19 Jul 2001.
- [8] R. Marconato, *Electric Power systems*, vol. 2, ISBN: 88-432-0025-9, CEI, 2004.
- [9] A. Berizzi, C. Bovo, M. Delfanti, M. Merlo, F. Tortello, *Singular Value Decomposition for an ORPF formulation in presence of SVR*, MELECON 2006. Malaga, Spain, 16-19 May.
- [10] W. Rosehart, C. Roman, A. Schellenberg, *Optimal Power Flow with complementary constraints*, IEEE Transactions on power systems, vol. 20, no. 2, May 2005.
- [11] A. Berizzi, C. Bovo, M. Innorta, P. Marannino, *Multiobjective optimization techniques applied to modern power systems*, IEEE PES Winter Meeting, Columbus (Ohio), USA. 28 January - 1 February 2001.
- [12] R. E. Rosenthal, *GAMS – a users guide*. [Online]. Available: www.gams.com
- [13] O. Schenk, K. Gaertner, *Solving unsymmetric sparse systems of linear equations with PARDISO*, Journal of Future Generation Computer Systems, vol 20, no. 3, pp. 475-487, 2004.
- [14] O. Schenk, K. Gaertner, *On fast factorization pivoting methods for sparse symmetric indefinite systems*, in Elec. Trans. Numer., vol 23, pp. 158-179, 2006.

VI. BIOGRAPHIES

Valentin Ilea received the B.S. degree in electric power systems engineering from the University “Politehnica” of Bucharest in 2006. Currently, he is a Ph.D. student involved in a double doctorate between University “Politehnica” of Bucharest and Politecnico di Milano.

His areas of research include power system analysis and optimization, power system dynamics and FACTS devices.



Cristian Bovo received his M.Sc. degree (1998) and his Ph.D. degree (2002) in Electrical Engineering from the Politecnico di Milano, where he is now Researcher at the Department of Energy.

His areas of research include power system analysis, voltage stability, and optimization and electricity markets.



Marco Merlo received the M.Sc. and Ph.D. degrees in Electrical Engineering both at the Politecnico di Milano in 1999 and in 2003 respectively. He is now Researcher at the Department of Energy of the Politecnico di Milano.

His areas of research include voltage stability, reactive scheduling, power system analysis and control, Artificial Intelligent techniques applied to power systems.



Alberto Berizzi received his M.Sc. degree (1990) and his Ph.D. degree (1994) both in Electrical Engineering from the Politecnico di Milano. He is now Professor at the Energy Department of the Politecnico di Milano.

His areas of research include power system analysis and optimization and power system dynamics.



Mircea Eremia (M’98, SM’02) received the B.S. and Ph.D. degree in electrical engineering from the Polytechnic Institute of Bucharest in 1968 and 1977 respectively.

He is currently Professor at the Electric Power Engineering Department from University “Politehnica” of Bucharest. His areas of research include transmission and distribution of electrical energy, power system stability and FACTS applications in power systems.

